# Nonequilibrium, Nonsimilar Solutions of the Laminar Boundary-Layer Equations

ADRIAN J. PALLONE,* JEFFREY A. MOORE,† and JOHN I. ERDOS‡
*Avco Corporation, Wilmington, Mass.*

**A method of solution of the laminar boundary-layer equations for dissociating and ionizing air in chemical nonequilibrium is formulated for arbitrary pressure gradients and body geometry. A nonsimilar, multistrip integral technique is employed in conjunction with previously derived transport and thermodynamic properties for the multicomponent mixture of pure-air species. The reaction rates are taken from recent experimental results. Several numerical examples are carried out for sharp conical bodies (assuming a fully-catalytic cold wall) at re-entry velocities and altitudes between 115 and 200 kft. The results are used to demonstrate a number of salient features of the flow fields; among these are the dominant role of diffusion in counterbalancing the production of dissociated and ionized species, the relative importance of precise transport properties in the momentum and energy equations for accurate prediction of observables such as electron density, and the persistence of chemical nonequilibrium to relatively low altitudes (below 115 kft) for slender, sharp vehicles at re-entry velocities.**

## Nomenclature

$C_p$ = specific heat at constant pressure
$\mathfrak{D}_{\alpha\beta}$ = binary diffusion coefficient
$D_{\alpha\beta}$ = multicomponent diffusion coefficient
$H$ = stagnation enthalpy of the mixture
$h_\alpha$ = enthalpy per unit mass of species $\alpha$, as referred to $O_2$ and $N_2$ at 0°K
$k_\alpha^{\mathrm{I}}$, $k_\alpha^{\mathrm{II}}$, $k_\alpha^{\mathrm{III}}$ = chemical reaction rate constants for species $\alpha$, referred to reaction I, II, or III, defined in Table 1
$k^{\mathrm{IV}}, \ldots k^{\mathrm{VII}}$ = "global" chemical reaction rate constants for the reactions IV to VII, defined in Table 1
$K_N^{\mathrm{I}} \ldots K_N^{\mathrm{VII}}$ = equilibrium constants for reactions I–VII
$M_\alpha$ = molecular weight of species $\alpha$
$\bar{M}$ = molecular weight of the gas mixture
$\dot{m}$ = mass flux per unit volume
$N_\alpha$ = number of moles of species $\alpha$ per unit volume
$n$ = exponent of the variable $\eta$ in the polynomials defining the velocity, enthalpy, and mass concentration functions ($n = 0, 1, 2, \ldots$)
$p$ = hydrostatic pressure
$r$ = local cylindrical body radius
$R_0$ = universal gas constant = 1.987 cal/g-mole-°K
$Re$ = Reynolds number based on the local properties at the outer edge of the boundary layer $= \rho_1 u_1 L/\mu_1$
$T$ = absolute temperature, °K
$u$ = $x$ component of the mass average velocity of the gas mixture
$v$ = $y$ component of the mass average velocity of the gas mixture
$W_\alpha$ = mass rate of formation of species $\alpha$ per unit volume due to chemical reactions
$X_\alpha$ = mole fraction of species $\alpha$, $= (N_\alpha/N)$
$x$ = coordinate along the surface
$Y_\alpha$ = mass fraction of species $\alpha$, $= \rho_\alpha/\rho$
$y$ = coordinate normal to surface
$z$ = positive integer which is identified with a given boundary-layer strip ($z = 1, 2, \ldots Z$)
$Z$ = total number of strips into which the boundary layer is divided
$\delta$ = boundary-layer thickness in the $(x$-$y)$ plane
$\eta$ = transformed variable
$\lambda_\beta$ = thermal conductivity of species $\beta$
$\lambda$ = thermal conductivity of the gas mixture
$\Lambda$ = nondimensional boundary-layer thickness parameter in the transformed plane
$\nu_\alpha$ = $y$ component of the average diffusion velocity of species $\alpha$
$\mu_\alpha$ = coefficient of viscosity of species $\alpha$
$\mu$ = coefficient of viscosity of the gas mixture
$\xi$ = transformed variable
$\rho_\alpha$ = mass density of species $\alpha$, $= N_\alpha M_\alpha$
$\rho$ = mass density of the gas mixture, $= N\bar{M}$

***Subscripts***

0 = value at the initial line
1 = value at the outer edge of the boundary layer
$\infty$ = value at infinity
$a, b, c, d, e, f$ = species subscript for $N_2$, N, $O_2$, O, NO, and $NO^+$, respectively
$s$ = stagnation value
$w$ = value at the body surface
$z$ = value at the outer boundary of strip $z$
$\alpha, \beta, \gamma$ = generalized subscripts referring to species $a, b, c, d$, and $e$
$x, y, \eta$ = partial differentiation with respect to the variable indicated

## Introduction

ACCURATE description of the re-entry environment of hypersonic vehicles (including quantitative evaluation of observables and communication capabilities) requires detailed analysis of the flow field, including "real gas" effects. The coupled chemical relaxation and diffusion phenomena are especially significant at hypervelocities, and their effects on the flow field are the subject of the present investigation.

A review of the general status of the theories of viscous dissociating gases (up to about two years ago) can be found in the texts of Hayes and Probstein[1] and Dorrance,[2] although most results presented are restricted to the limiting cases of either frozen (nonreacting) or equilibrium air flows. Some of the more recent work on nonequilibrium air boundary layers is contained in Refs. 3–8 (although these are not in-

Presented as Preprint 64-40 at the AIAA Aerospace Sciences Meeting, New York, January 20–22, 1964; revision received June 9, 1964. The authors acknowledge with pleasure the excellent work and perseverence of William Spendiff of the Mathematics Section at Avco/RAD in developing the computer program used in these studies.

* Manager, Aerophysics Department.
† Senior Scientist; now at the University of Buffalo, Buffalo, N. Y. Member AIAA.
‡ Senior Scientist. Member AIAA.

tended to comprise a complete bibliography of significant research in this area).

In the present paper, the laminar boundary-layer flow of dissociated air in chemical nonequilibrium is formulated for arbitrary pressure gradients and body geometries. The aim is to extend the multistrip integral techniques§ to obtain high-order approximate solutions for a generalized model of the nonequilibrium boundary layer. The method will permit more exact determination of the boundary-layer characteristics (including species concentration, velocity, and temperature profiles) and also will serve to check results obtained by simpler approaches. The main emphasis of this study will be on dissociation and ionization nonequilibrium.

Related phenomena such as vibration-dissociation coupling, and radiative transfer will be neglected. Viscous-inviscid interaction (however important at the high altitudes) will also be neglected at this time so as to more clearly emphasize the primary effects.

The air model adopted for the present analysis considers a seven-component gas mixture (O, $O_2$, N, $N_2$, NO, $NO^+$, $e^-$), with the molecular internal degrees of freedom in equilibrium with the translational mode. The ionization reaction is uncoupled from the other six (dissociation) reactions; i.e., the ionization energy is assumed negligible. The most recent reaction rates are employed (Lin and Teare[11]) in conjunction with newly derived transport and thermodynamic properties (to 10,000°K.)[3]

## Basic Equations

The classical boundary-layer approximations are employed in simplifying the governing equations (e.g., Refs. 12 and 13) for the viscous flow of a chemically reacting, multicomponent gas mixture. For steady laminar flow, the resulting set of general expressions of mass, momentum, energy, and species conservation are the following:

$$(\rho u r^j)_x + (\rho v r^j)_y = 0 \tag{1}$$

$$\rho u u_x + \rho v u_y = -P_x + (\mu u_y)_y \tag{2}$$

$$0 = P_y \tag{3}$$

$$\rho u H_x + \rho v H_y = \left\{ \mu \left[ \frac{\lambda}{\mu} (T_s)_y + \left(1 - \frac{\lambda}{c_{p_1}\mu}\right)\left(\frac{u^2}{2}\right)_y \right] - \sum_\alpha \rho Y_\alpha \nu_\alpha h_\alpha \right\} \tag{4}$$

$$\rho u (Y_\alpha)_x + \rho v (Y_\alpha)_y = W_\alpha - (\rho Y_\alpha \nu_\alpha)_y \tag{5}$$

where

$$Y_\alpha \nu_\alpha = \sum_\beta D_{\alpha\beta} \left[ \frac{M_\alpha}{\bar{M}} (Y_\beta)_y - Y_\beta \left(\frac{M_\alpha}{\bar{M}}\right)_y \right]$$

$$j = \begin{cases} 0 \text{ for planar body} \\ 1 \text{ for axisymmetric body} \end{cases}$$

$$T_s \equiv T + (u^2/2C_{p_1})$$

The gas mixture is postulated to be sufficiently dilute to allow each chemical species to be treated as an ideal gas, i.e.,

$$P_\alpha = \rho_\alpha (R_0/M_\alpha) T \tag{6}$$

For the mixture,

$$P = \rho (R_0/\bar{M}) T \tag{7}$$

where

$$\bar{M} = \sum_\alpha X_\alpha M_\alpha = \left[ \sum_\alpha (Y_\alpha/M_\alpha) \right]^{-1}$$

§ The integral technique employed in this study has been developed in previous boundary-layer and wake studies with equilibrium air (Pallone[9] and Pallone, Erdos, and Eckerman[10]).

The boundary conditions on velocity and enthalpy are those usually imposed on the boundary layer, namely,

$$\left.\begin{aligned} u &= u_1, & u_y &= 0 \\ H &= H_1, & H_y &= 0 \end{aligned}\right\} y = \delta$$

and

$$\left.\begin{aligned} u &= 0, \\ H &= H_w \text{ or } H_y = (H_y)_w \end{aligned}\right\} y = 0$$

The boundary conditions on the species concentration at the outer edge of the layer are¶

$$Y_\alpha = Y_{\alpha_1} \qquad (Y_\alpha)_y = 0 \qquad (y = \delta)$$

However, the boundary conditions at the wall are dictated by the degree of catalycity of the wall material. Although the detailed kinetics of catalytic recombination at a surface are not yet well defined for a multicomponent gas mixture, the following formulation, which considers only the limiting cases of a noncatalytic or a fully catalytic surface (an extension of the binary mixture work of Goulard[14]) is proposed for the present analysis.

At the wall, with no injection, the net mass flux of species $\alpha$ toward the wall is due only to diffusion, and may be described by:

$$\dot{m}_\alpha = -\rho_w (Y_\alpha \nu_\alpha)_w \tag{8}$$

The mass flux is precisely balanced by the recombination at the wall, which can be assumed, for example, to be a first-order process:

$$\dot{m}_\alpha = k_\alpha (Y_\alpha \rho_\alpha)_w \qquad (\alpha = b, d, e, f) \tag{9}$$

The flux of the molecular species $N_2$ and $O_2$ is given from consideration of species conservation

$$2\frac{\dot{m}_{O_2}}{M_{O_2}} = -\left[\frac{\dot{m}_O}{M_O} + \frac{\dot{m}_{NO}}{M_{NO}} + \frac{\dot{m}_{NO^+}}{M_{NO^+}}\right] \tag{10}$$

$$2\frac{\dot{m}_{N_2}}{M_{N_2}} = -\left[\frac{\dot{m}_N}{M_N} + \frac{\dot{m}_{NO}}{M_{NO}} + \frac{\dot{m}_{NO^+}}{M_{NO^+}}\right] \tag{11}$$

$$\sum_\alpha Y_\alpha = 1$$

Clearly, in the noncatalytic case ($k_\alpha = 0$), the species boundary conditions at the wall become

$$(\partial Y_\alpha/\partial y)_w = 0 \tag{12}$$

However, in the fully catalytic case ($k_\alpha = \infty$), the mass flux is bounded and therefore,

$$Y_{\alpha w} = 0 \qquad (\alpha = b, d, e, f) \tag{13}$$

The values of $Y_{N_2}$ and $Y_{O_2}$, at the surface, are controlled by (multicomponent) diffusion, through which all the species are coupled. The boundary conditions on the $N_2$ and $O_2$ are as determined by Eqs. (8, 9, 11, and 13). In the examples selected for the present paper, only the fully catalytic case was considered. The boundary conditions given by Eq. (13) are used, and, to avoid the numerical difficulties associated with coupling of the species equations, the concentrations of $N_2$ and $O_2$ at the surface are assumed to be the same as at the outer edge of the boundary layer.** A

¶ The velocity, enthalpy, and species concentrations are assumed to have the same thickness, but the enthalpy and concentration profiles are allowed an additional free coefficient in the polynomial formulas (see "Method of Analysis") to compensate for this restriction. These coefficients are related to the wall gradients of the enthalpy and concentrations, which replace their thicknesses as unknowns. This procedure is discussed in Ref. 9.

** Both the wall and outer edge temperatures are less than 1000°K in the examples.

**Table 1 Rate constants for chemical processes**

| No. | Reaction | Third body (p) | Exothermic rate constant |
|---|---|---|---|
| I | $O_2 + (p) + 5.1$ ev $\rightleftarrows 2O + (p)$ | N, NO | $k_b^{I} = k_e^{I} = 3.01 \times 10^{15} \times T^{-1/2}$ |
| | | $N_2$ | $k_a^{1} = 2k_b^{1}$ |
| | | $O_2$ | $k_c^{I} = 8.0 \times 10^{19} \times T^{-3/2}$ |
| | | O | $k_d^{I} = 2.8\, k_c^{1}$ |
| II | $N_2 + (p) + 9.8$ ev $\rightleftarrows 2N + (p)$ | O, $O_2$, NO | $k_c^{II} = k_d^{II} = k_e^{II} = 0.395\, k_a^{II}$ |
| | | $N_2$ | $k_a^{II} = 2.76 \times 10^{16} \times T^{-1/2}$ |
| | | N | $k_b^{II} = 2.36 \times 10^{21} \times T^{-3/2}$ |
| III | $NO + (p) + 6.5$ ev $\rightleftarrows N + O + (p)$ | $O_2$, $N_2$, | $k_a^{III} = k_b^{111} = k_c^{111} = k_d^{III}$ |
| | | O, N | $= 1.02 \times 10^{20} \times T^{-3/2}$ |
| | | NO | $20\, k_a^{III}$ |
| IV | $NO + O + 1.4$ ev $\rightleftarrows O_2 + N$ | ... | $k^{IV} = 1.33 \times 10^{10} \times T \times e^{-3569/T}$ |
| V | $N_2 + O + 3.3$ ev $\rightleftarrows NO + N$ | ... | $k^{V} = 1.63 \times 10^{13}$ |
| VI | $N_2 + O_2 + 1.9$ ev $\rightleftarrows 2NO$ | ... | $k^{VI} = 2.41 \times 10^{23} \times T^{-5/2} \times e^{-43,000/T}$ |
| VII | $N + O + 2.8$ ev $\rightleftarrows NO^+ + e^-$ | ... | $k^{VIII} = 1.81 \times 10^{21} \times T^{-3/2}$ |

posteriori, this assumption is justified due to the very slight dissociation of $N_2$ encountered.

## Transport Properties, Thermodynamics, and Chemistry

Extensive calculations have been made by Bade of the species viscosity, thermal conductivity, and pertinent binary diffusion coefficients, as functions of temperature. These computations and the complete multicomponent formalism used for computing the transport properties of the mixture are summarized in Appendix B of Ref. 3. The thermodynamic properties of the species and the mixture are calculated by the usual procedures of statistical mechanics, assuming the internal degrees of freedom of the molecules to be in equilibrium with the translational mode.††

The significant gas-phase reactions for high-temperature air are taken to be the seven given in Table 1. Unless specified otherwise, the reaction rates used in the calculations are the most recent given by Lin and Teare.[11]

The net rate of production of each chemical species is dictated by the (phenomenological) law of mass action, with the appropriate (experimental) reaction rates. The species "source" equations are written as in Ref. 3, with the following additional reaction included for the production of ions:

$$\frac{W_{NO^+}}{M_{NO^+}} = \frac{\partial N_{NO^+}}{\partial t} = -\frac{k^{VII}}{K_N{}^{VIII}}\left(N^2{}_{NO^+} - N_N N_O K_N{}^{VII}\right) \quad (14)$$

The equilibrium constants $K_n{}^{1}, \ldots, K_n{}^{VII}$ are known functions of temperature (utilizing the thermodynamic model described previously).‡‡

## Method of Analysis

The basic equations given previously (1–5) are reduced to a set of ordinary, first-order differential equations by employing a technique suggested by Dorodnitsyn's "method of integral relations."[16] Application of this technique to boundary-layer problems was described by Pallone[9] in a study of downstream effects of transpiration. The reader is referred to these papers for a more complete discussion of the method than is presented here.

The essence of the method lies in the division of the viscous domain into an arbitrary number of curvilinear strips $z$ in the streamwise direction, between the wall and an outer edge $\delta$. The boundary $\delta$ is identifiable as the physical boundary-layer thickness (of the velocity, thermal, and species profiles) where the condition from the inviscid flow are imposed. The basic equations are integrated with respect to $y$ from the wall to the edge of each strip. Polynomial expressions for $u$, $H$, and $Y_\alpha$ are introduced, where these variables appear in the integrals, with the polynomial coefficients required to satisfy the boundary conditions and the values of the functions on the strip boundaries. An extra, free coefficient is allowed in the enthalpy and species profiles (to compensate for restricting all the profiles to a single thickness). A density (Howarth-Dorodnitsyn) transformation is employed, and the strip boundaries are fixed in the transformed plane, i.e.,

$$\eta\delta_t = \int_0^y \frac{\rho}{\rho_1}\, dy \quad (15)$$

$$\xi = x/L \quad (16)$$

where

$$\delta_t = \int_0^\delta \frac{\rho}{\rho_1}\, dy$$

$$\eta_k = \frac{1}{\delta_t}\int_0^{y_k} \frac{\rho}{\rho_1}\, dy = \frac{Z - (k-1)}{Z} \qquad (k = 1, 2, \ldots, Z)$$

The following set of ordinary differential equations is thereby derived:

$$F_{1k}\frac{d\Lambda}{3\xi} + \Lambda\frac{dF_{1k}}{d\xi} - \Lambda F_{2k}\frac{d}{d\xi}\left(\frac{u_k}{u_1}\right) + (l_k\tau_k - l_w\tau_w) = -\Lambda\left[F_{1k}\frac{d}{d\xi}\ln(\rho_1 u_1 \mu_1)^{1/2} + \left(F_{1k} - \frac{u_k}{u_1}F_{2k} + F_{3k}\right)\frac{d\ln u_1}{d\xi} + j\frac{d\ln r}{d\xi}\right] \quad (17)$$

$$F_{4k}\frac{d\Lambda}{d\xi} + \Lambda\frac{dF_{4k}}{d\xi} - \Lambda F_{2k}\frac{d}{d\xi}\left(\frac{H_k}{H_1}\right) + \left[l\left\{\frac{T_{s1}}{H_1}\frac{\lambda}{\mu}\left(\frac{T_s}{T_{s1}}\right)_\eta + \left(1 - \frac{\lambda}{C_{p1}\mu}\right)\frac{u_1{}^2}{H_1}\left(\frac{u}{u_1}\right)\left(\frac{u}{u_1}\right)_\eta - \frac{\rho}{\mu}\sum_\alpha\frac{h_\alpha}{H_1}\sum_\beta D_{\alpha\beta}\left[\frac{M_\alpha}{\bar{M}}(Y_\beta)_\eta - Y_\beta\left(\frac{M_\alpha}{\bar{M}}\right)_\eta\right]\right\}\right]_w^k = -\Lambda F_{4k}\frac{d}{d\xi}\left[\ln(\rho_1 u_1 \mu_1)^{1/2} + j\ln r\right] \quad (18)$$

$$F_{5k}{}^{\alpha}\frac{d\Lambda}{d\xi} + \Lambda\frac{dF_{5k}{}^{\alpha}}{d\xi} - \Lambda F_{2k}\frac{dY_\alpha}{d\xi} + \Lambda F_{6k}{}^{\alpha} + \left\{\frac{\rho}{\mu}\sum_\beta D_{\alpha\beta}\left[\frac{M_\alpha}{\bar{M}}(Y_\beta)_\eta - Y_\beta\left(\frac{M_\alpha}{\bar{M}}\right)_\eta\right]\right\}_w^k = -\Lambda F_{5k}{}^{\alpha}\frac{d}{d\xi}\left[\ln(\rho_1 u_1 \mu_1)^{1/2} + j\ln r\right] \quad (19)$$

†† The electron diffusion is assumed to be described by a binary diffusion coefficient for electron-ion pairs through air molecules, i.e., $\mathfrak{D}_{fa} = 2\mathfrak{D}_{ea}$.

‡‡ The equilibrium constants given by Wray[15] follow very closely those employed here.

where:

$$\Lambda = \frac{\rho_1 u_1 L}{\mu_1}\left(\frac{\delta_t}{L}\right)^2 \qquad \tau = \left(\frac{u}{u_1}\right)_\eta$$

$$\alpha = \left(\frac{H}{H_1}\right)_\eta \qquad l = \frac{\rho\mu}{\rho_1\mu_1}$$

$$F_{1_k} = \int_0^{\eta_k} \frac{u}{u_1}\left(\frac{u_k}{u_1} - \frac{u}{u_1}\right) d\eta$$

$$F_{2_k} = \int_0^{\eta_k} \frac{u}{u_1}\, d\eta$$

$$F_{3_k} = \int_0^{\eta_k} \left(\frac{\rho}{\rho_1}\right)^{-1} d\eta$$

$$F_{4_k} = \int_0^{\eta_k} \frac{u}{u_1}\left(\frac{H_k}{H_1} - \frac{H}{H_1}\right) d\eta$$

$$F_{5_k}{}^{\alpha} = \int_0^{\eta_k} \frac{u}{u_1}\,(Y_{\alpha_k} - Y_\alpha)\, d\eta$$

$$F_{6_k}{}^{\alpha} = \int_0^{\eta_k} \left(\frac{\rho}{\rho_1}\right)^{-1} \frac{W_\alpha}{\rho_1 u_1 L}\, d\eta$$

The integration of the $F$ integrals is carried out by using

$$\frac{u}{u_1} = \sum_{n=0}^{z+1} a_n \eta^n \qquad a_n = a_n\left[\eta_k, \frac{u_k}{u_1}\right]$$

$$\frac{H}{H_1} = \sum_{n=0}^{z+2} b_n \eta^n \qquad b_n = b_n\left[\eta_k, \frac{H_k}{H_1}, \left(\frac{\partial H_k/H_1}{\partial\eta}\right)_w\right]$$

$$Y_\alpha = \sum_{n=0}^{z+2} c_n \eta^n \qquad c_n = c_n\left[\eta_k, Y_{\alpha_k}, \left(\frac{\partial Y_\alpha}{\partial\eta}\right)_w\right]$$

Moreover, the values of $\rho_k$, $W_{\alpha_k}$, $\bar{M}_k$, $T_{s_k}$, etc., can be computed from the dependent variables $u_k$, $H_k$, and $Y_{\alpha_k}$, along a line $\xi$ = const preceding each $\Delta\xi$ integration step. For example, the static temperature is calculated from the mixture enthalpy and species concentrations by utilizing tabulations of species enthalpy as a function of temperature.[3] The static temperature, in turn, dictates the transport properties of the species and thus of the mixture.

Equations (17–19) therefore constitute a set of algebraic relations for the derivatives of $u_k$, $H_k$, $Y_{\alpha k}$, $H_w$ or $(H\eta)_w$, and $Y_{\alpha u}$, or $(Y_{\alpha\eta})_w$, which are integrated numerically from a set of initial values of the dependent variables. The integration is carried out by a predictor-corrector method.[17]

## Presentation and Discussion of Results

The example presented in this section is chosen with a dual purpose: first, to display some of the essential features of nonequilibrium boundary-layer flow (including effects of reaction rates and transport and thermodynamic properties); second, to provide practical information required for a better understanding of the re-entry environment of hypersonic vehicles. The following case has been selected for detailed study: 8°-half-angle cone, 15-ft length, $u_\infty$ = 22,000 fps, alt = 200, 150, and 115,000 ft, "fully catalytic" wall, at $T_w$ = 1000°K.

The influence of diffusion (including an evaluation of the binary diffusion approximation) and the effect of an alternate set of reaction rates are examined at the 150,000 ft alt only. The altitude effects are studied separately with the latest reaction rates (see Table 1) and multicomponent diffusion.

The flow is assumed chemically frozen for the first 6 in. from the cone apex (which is assumed to be sharp). A similar solution[18] is employed to describe the boundary layer at $x$ = 0.5 ft, which is taken as the initial condition for the present analysis. The initial velocity and temperature profiles are shown in Figs. 1 and 2. The mixture Prandtl number ($PR$) is close to 0.75; the $PR$ = 1.0 and Blasius results are shown for comparison.

The streamwise variation of the peak values of the atomic oxygen concentration, nitric oxide concentration, and electron density at 150,000 ft, as computed from the present analysis, are shown in Figs. 3–5. The results 1) from an

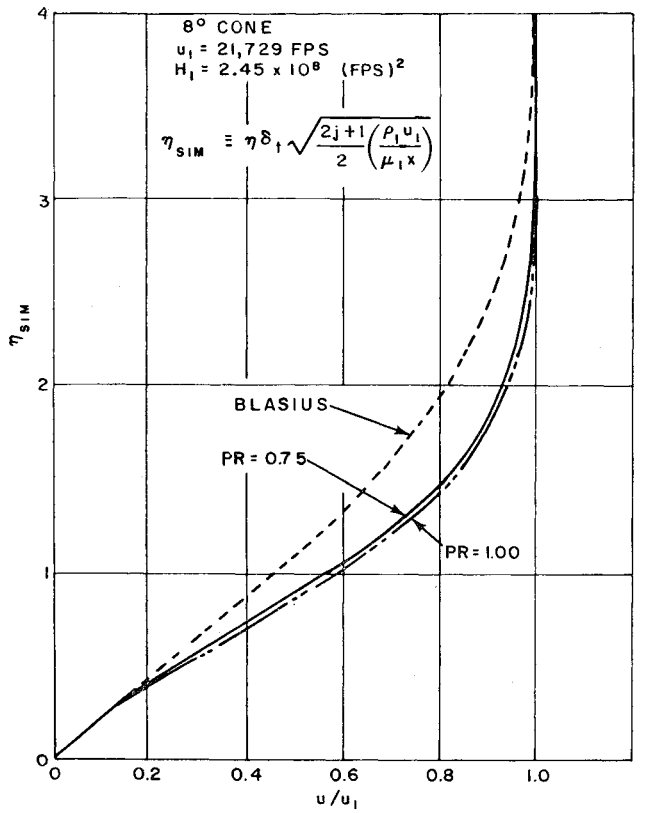


**Fig. 1 Initial velocity profile, from similarity solution for frozen chemistry and vibrational equilibrium.**

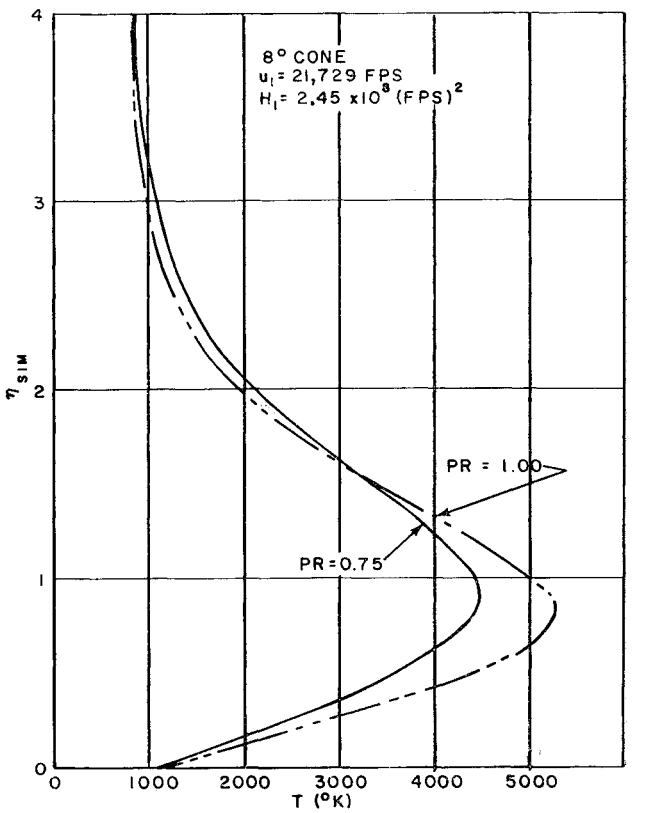


**Fig. 2 Initial temperature profile, from similarity solution for frozen chemistry and vibrational equilibrium.**

alternate set of reaction rates,[19] 2) neglecting diffusion velocity, and 3) holding the velocity and enthalpy profiles fixed as well as neglecting diffusion (i.e., the "streamtube-type" approximation), in addition to 4) the basic results with multicomponent diffusion coefficients, are illustrated in these figures. The results of streamtube calculations[20] with both $PR = 0.75$ and $PR = 1.0$ initial conditions are also shown. It should be noted that diffusion accounts for about an order-of-magnitude drop in the atomic nitrogen (not illustrated here) and atomic oxygen concentrations at 15 ft, more than an order-of-magnitude drop in the peak nitric oxide concen-

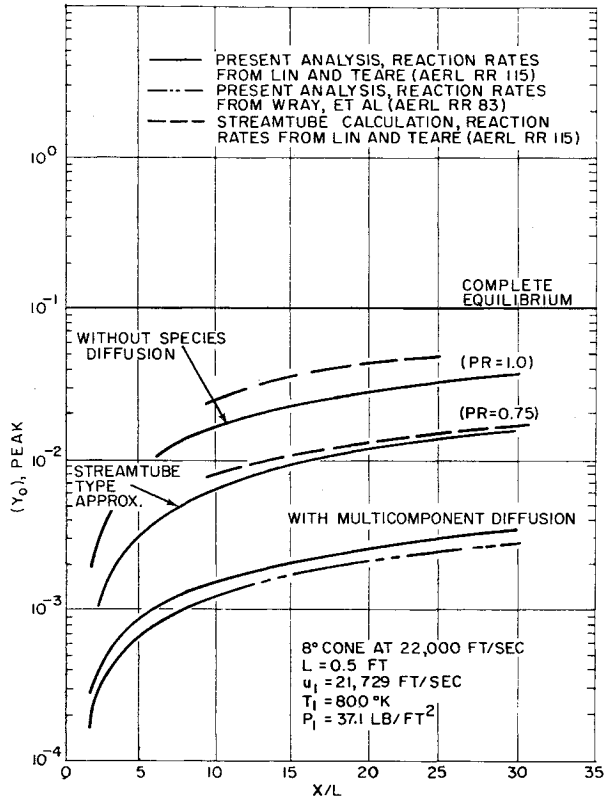


**Fig. 3 Nonequilibrium peak O concentration at 150,000-ft alt.**

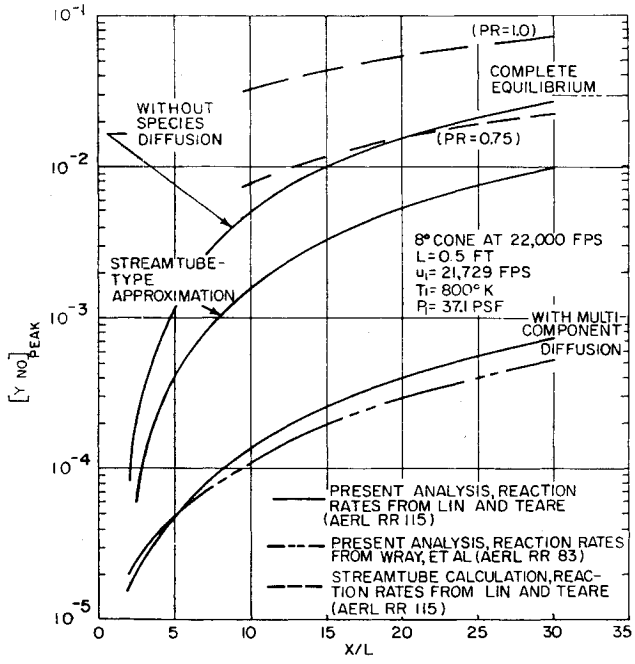


**Fig. 4 Nonequilibrium peak NO concentration at 150,000-ft alt.**

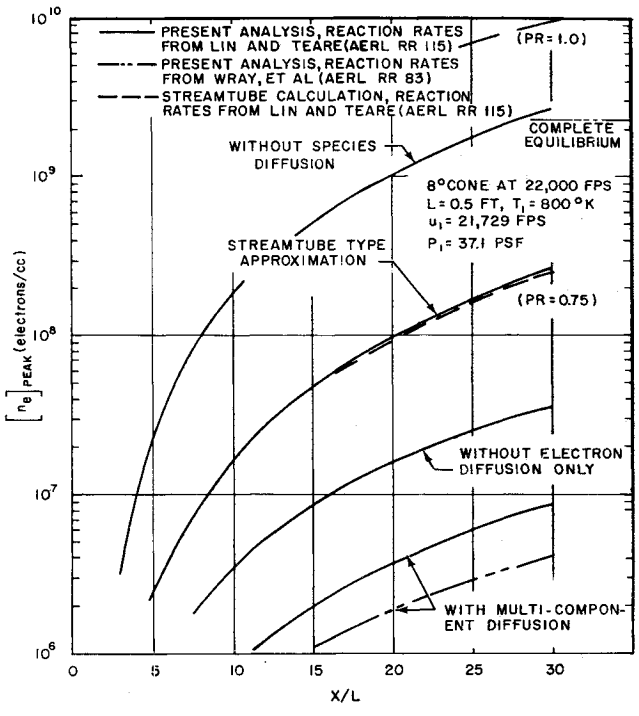


**Fig. 5 Nonequilibrium peak electron density at 150,000-ft alt.**

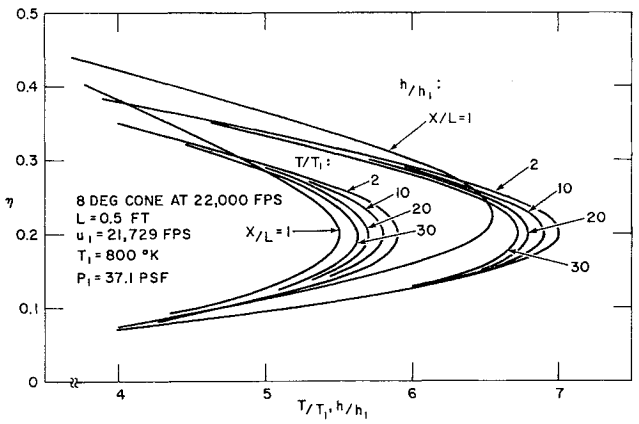


**Fig. 6 Nonequilibrium temperature and enthalpy profiles at 150,000-ft alt (present analysis, including multicomponent species diffusion).**

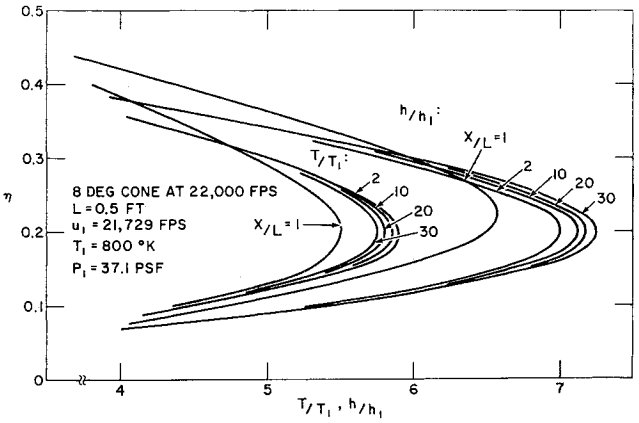


**Fig. 7 Nonequilibrium temperature and enthalpy profiles at 150,000-ft alt (present analysis without species diffusion).**

tration, and more than two orders-of-magnitude decrease in electron density. However, as shown in Fig. 5, neglect of the electron diffusion alone results in only a factor of four increase from the electron density computed with diffusion of all species, i.e., the electron density is primarily dictated by the concentrations of N and O present, and diffusion of the electron-ion pairs per se is secondary.

Typical temperature and enthalpy profiles at 150,000 ft are shown in Figs. 6 and 7. It may be seen that with species diffusion, the peak enthalpy is reduced by dissociation (a Lewis number effect), whereas without species diffusion (or with $LE = 1$) the peak enthalpy increases slightly. It should be noted that in the streamtube approximation the enthalpy is invariant. Some typical profiles of atomic oxygen and nitric oxide concentration and electron density are shown in Figs. 8–10, to illustrate more clearly the diffusion effect. Also, the use of a binary diffusion coefficient (the N-$N_2$ coefficient in this case) is shown to be adequate in the present example.

The effect of altitude on the nonequilibrium viscous flow field is indicated by the streamwise variations in the peak values of the concentrations of atomic oxygen and nitric oxide, and electron density shown in Figs. 11–13. Typical profiles of temperature, concentration of atomic oxygen and nitric oxide, and electron density are illustrated in Figs. 14–17.

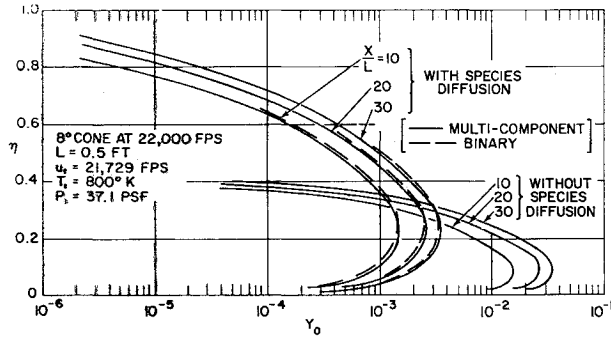


**Fig. 8 Typical O concentration profiles at 150,000-ft alt.**

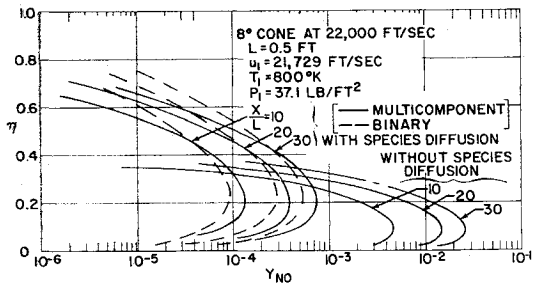


**Fig. 9 Typical NO concentration profiles at 150,000-ft alt.**

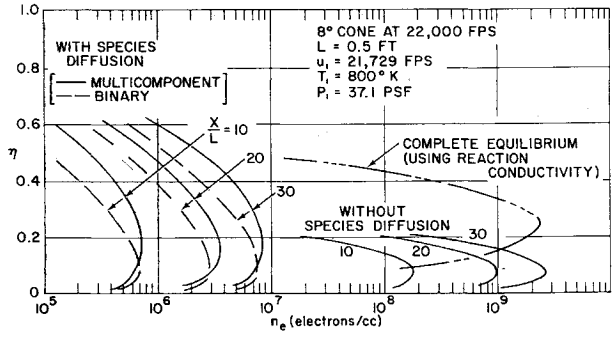


**Fig. 10 Typical electron density profiles at 150,000-ft alt.**

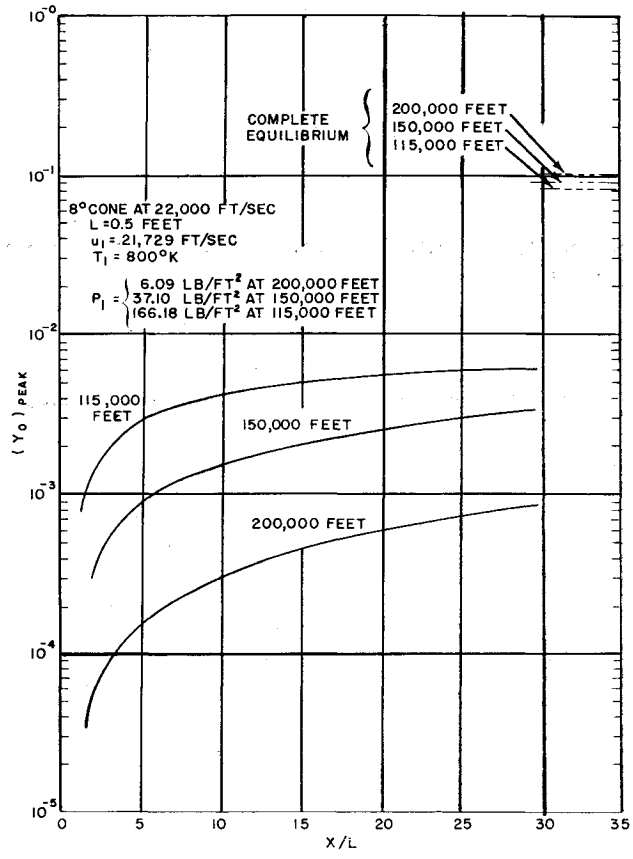


**Fig. 11 Effect of altitude on growth of peak O concentration.**

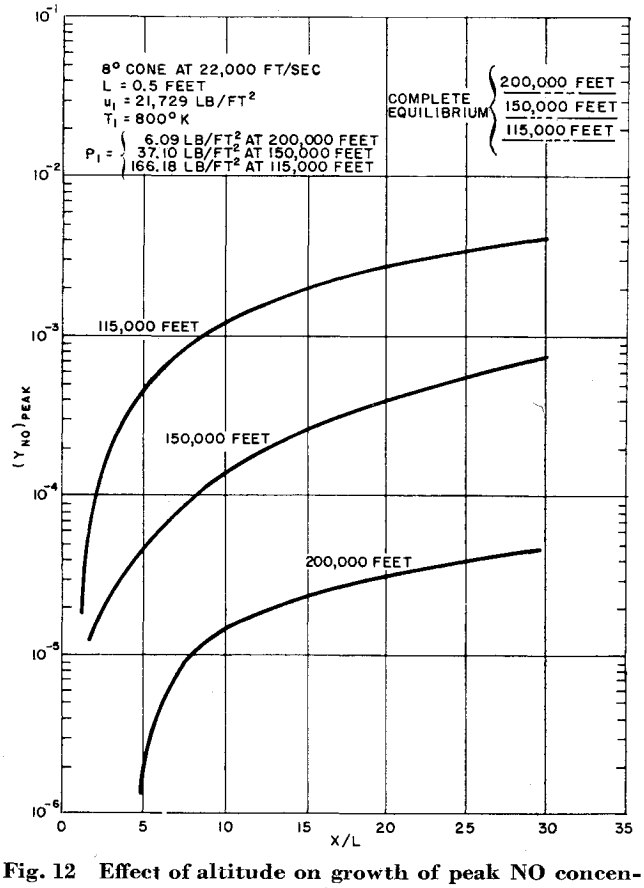


**Fig. 12 Effect of altitude on growth of peak NO concentration.**

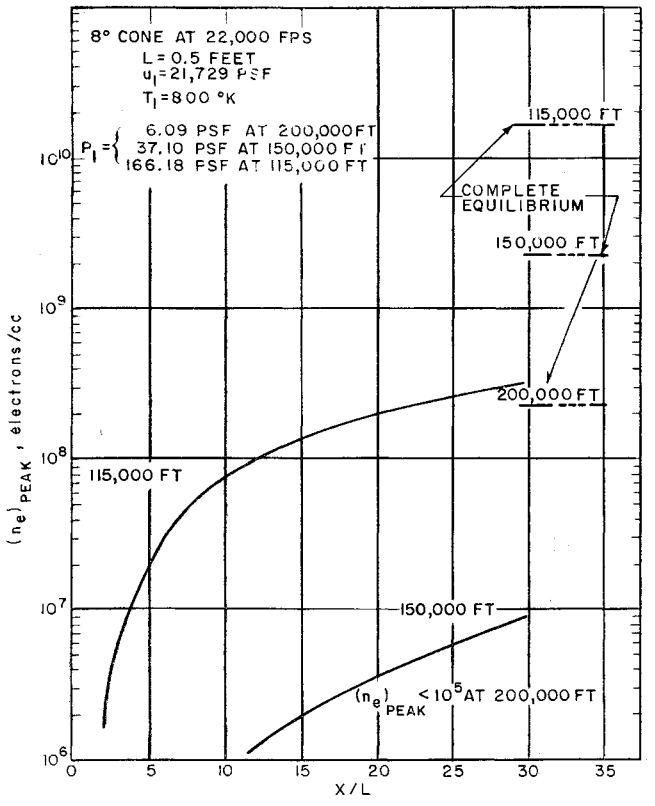


**Fig. 13 Effect of altitude on growth of peak electron density.**

The inverse transformation necessary to convert the normal coordinate $\eta$ used in many of the figures to the physical distance $y$ is indicated in Fig. 18.

## Binary Scaling

Gibson[21] has pointed out that the binary scaling parameter $\rho_\infty x/u_\infty$, preserves the Reynolds number for a given vehicle velocity and geometry, and therefore is appropriate for viscous, as well as inviscid flows. Further attention has been given to the development of binary scaling laws by Levinsky and Fernandez[22] who have compared the present results with those obtained by Blottner[8] by a finite-difference technique. The electron density (the quantity of primary interest) presented here begins to deviate from the binary collision model at about $X > 5$ ft at the 115,000 ft alt,[22] but Blottner's results follow this model to $X = 15$ ft at 100,000 ft (for a 10° cone at 22,000 fps).[8] The precise cause of this difference is particularly difficult to isolate in a multicomponent, reacting mixture problem; there are, for example, differences in the transport and thermodynamic properties used for pure species, as well as in the reaction kinetics and rates. However, it has been shown[7] that the two methods of analysis given essentially the same results for a binary mixture with consistent thermodynamics, transport properties, and reaction rates.

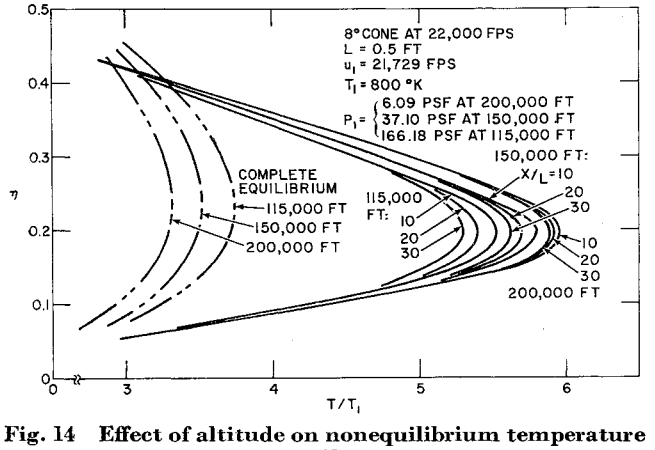


**Fig. 14 Effect of altitude on nonequilibrium temperature profiles.**

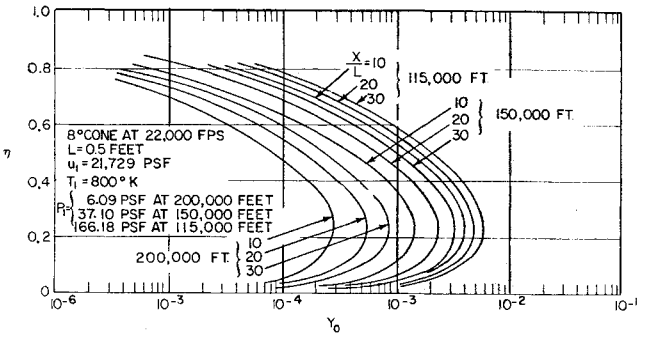


**Fig. 15 Effect of altitude on nonequilibrium O concentration profiles.**

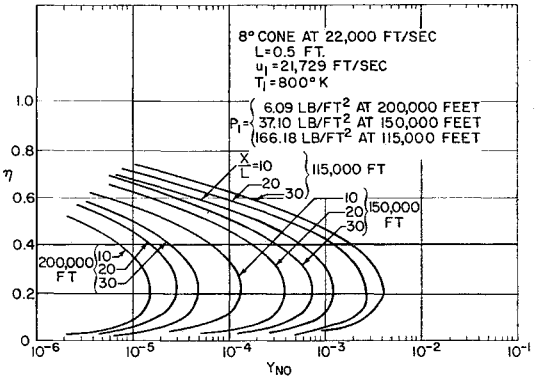


**Fig. 16 Effect of altitude on nonequilibrium NO concentration profiles.**

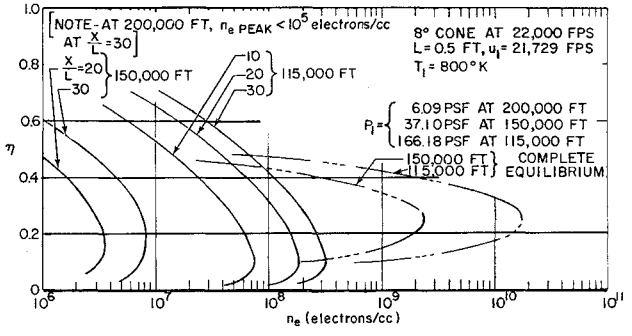


**Fig. 17 Effect of altitude on nonequilibrium electron density profiles.**

## Conclusions

The following conclusions are drawn from the present study:

1) Diffusion in the nonequilibrium laminar boundary-layer flow over a fully catalytic wall plays a dominant role in determining the species concentrations (including electrons). The "streamtube approximation,"[20] although offering appealing simplicity, can give only qualitative trends with any reliability. Further study is required to evaluate the diffusion effects with noncatalytic or partially catalytic surfaces, or at substantially higher temperatures ($T > 5000$°K).

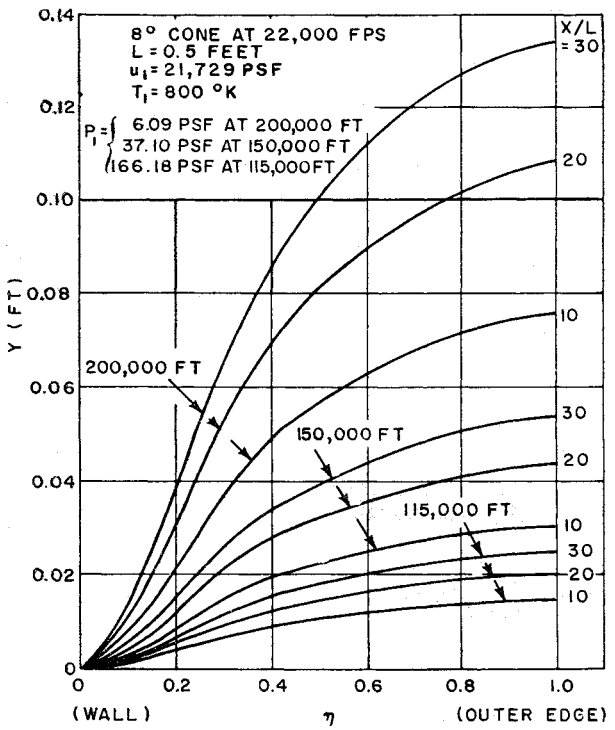


**Fig. 18 Inverse transformation (from incompressible to physical plane).**

2) Major differences in concentrations (e.g., an order-of-magnitude in electron density) can result from seemingly slight enthalpy variations. The importance of accurate transport and thermodynamic properties of the nonequilibrium mixture must be emphasized in this regard. However, the use of a binary diffusion coefficient (rather than the multicomponent coefficients) was found to give satisfactory results at 150,000 ft. It appears that this may be a useful approximation wherever one species clearly overshadows the rest in the composition of the mixture ($N_2$ is the dominant species in this case), but this may be justified only a posteriori.

3) Nonequilibrium chemistry in the boundary layer persists to relatively low altitudes (less than 115,000 ft) for slender, sharp vehicles at re-entry velocities.

4) The present results are consistent with binary scaling up to $X \approx 5$ ft at an altitude of 115,000 ft. An appreciable deviation from the binary collision model occurs by $X \approx 15$ ft at this altitude, and it appears the problem of partial equilibrium may require examination for lower altitudes.

## References

[1] Hayes, W. D. and Probstein, R. F., *Hypersonic Flow Theory* (Academic Press, New York, 1959), Chap. 8.

[2] Dorrance, W. H., *Viscous Hypersonic Flow* (McGraw-Hill Book Co., Inc., New York, 1962), Chaps. 4 and 5.

[3] Pallone, A. and Moore, J. A., "Similar solutions to the laminar boundary layer equations for nonequilibrium air," Avco/RAD TR 62-59 (July 1962).

[4] Inger, G. R., "Nonequilibrium stagnation point boundary layers with arbitrary surface catalycity," AIAA J. **1**, 1776–1783 (1963).

[5] Hartunian, R. A. and Thompson, W. P., "Nonequilibrium stagnation point heat transfer including surface catalysis," AIAA Preprint 63-464 (August 1963).

[6] Brainerd, J. J. and Levinsky, E. S., "Viscous and nonviscous nonequilibrium nozzle flows," AIAA J. **1**, 2474–2481 (1963).

[7] Pallone, A., Moore, J., and Erdos, J., "Nonequilibrium, nonsimilar solutions of the laminar boundary layer equations," AIAA Preprint 64-40 (January 1964).

[8] Blottner, F. G., "Nonequilibrium laminar boundary layer flow of ionized air," AIAA Preprint 64-41 (January 1964).

[9] Pallone, A., "Nonsimilar solutions of the compressible laminar boundary layer equations with application to the upstream transpiration cooling problem," J. Aerospace Sci. **28**, 449–456 (1961).

[10] Pallone, A., Erdos, J., and Eckerman, J., "Hypersonic laminar wakes and transition studies," AIAA J. **2**, 855–863 (1964).

[11] Lin, S. C. and Teare, J. D., "Rate of ionization behind shock waves in air," Avco-Everett Research Lab. Research Rept. 115 (September 1962).

[12] Hirschfelder, J. O., Curtiss, C. F., and Bird, R. B., *Molecular Theory of Gases and Liquids* (John Wiley and Sons, Inc., New York, 1954), p. 698.

[13] Penner, S. S., *Chemistry Problems in Jet Propulsion* (Pergamon Press, New York, 1957), p. 217.

[14] Goulard, R., "On catalytic recombination rates in hypersonic stagnation heat transfer," Jet Propulsion **28**, 737–745 (1958).

[15] Wray, K. L., "Chemical kinetics of high temperature air," *Progress in Astronautics and Rocketry: Hypersonic Flow Research*, edited by F. R. Riddell (Academic Press, New York, 1962), Vol. 7, pp. 181–204.

[16] Dorodnitsyn, A. A., "General method of integral relations and its application to boundary layer theory," *Advances In Aeronautical Sciences* (Macmillan Co., New York, 1962), Vol. 3, pp. 207–219.

[17] Katz, I. N., Morrissette, L. N., and Warga, J., "A space trajectory program," Avco/RAD TM-61-10, Sec. III (May 2, 1961).

[18] Van Tassell, W. and Pallone, A., "Similar solutions of the compressible laminar boundary layer equations for air in equilibrium dissociation and ionization with and without air injection in the stagnation region," Avco/RAD TM-61-22 (June 1961).

[19] Wray, K., Teare, J. D., Kivel, B., and Hammerling, P., "Relaxation processes and reaction rates behind shock fronts in air and component gases," Avco-Everett Research Lab., Research Rept. 83 (December 1959).

[20] DeRienzo, P., Wood, A., Berner, F., and Teare, J., "Effects of nonequilibrium on the hypersonic laminar boundary layer," *Proceedings of the Eighth Symposium on Ballistic Missile and Space Technology* (October 16–18, 1963); also published as Avco TM 64-2 (January 31, 1964); unclassified.

[21] Gibson, W. E., "Dissociation scaling for nonequilibrium blunt nose flows," ARS J. **32**, 285 (1962).

[22] Levinsky, E. S. and Fernandez, F. L., "Approximate nonequilibrium air ionization in hypersonic flows over sharp cones," AIAA J. **2**, 565–567 (1964).